



IceBridge MCoRDS L1B Geolocated Radar Echo Strength Profiles, Version 1

USER GUIDE

How to Cite These Data

As a condition of using these data, you must include a citation:

Leuschen, C. 2011, updated 2013. *IceBridge MCoRDS L1B Geolocated Radar Echo Strength Profiles, Version 1*. [Indicate subset used]. Boulder, Colorado USA. NASA National Snow and Ice Data Center Distributed Active Archive Center. <https://doi.org/10.5067/WVDXEKH0X7N3>. [Date Accessed].

FOR QUESTIONS ABOUT THESE DATA, CONTACT NSIDC@NSIDC.ORG

FOR CURRENT INFORMATION, VISIT <https://nsidc.org/data/IRMCR1B>



National Snow and Ice Data Center

TABLE OF CONTENTS

1	DETAILED DATA DESCRIPTION.....	2
1.1	Format	2
1.2	File and Directory Structure.....	2
1.3	File Naming Convention	3
1.4	File Size.....	3
1.5	Volume	3
1.6	Spatial Coverage.....	3
1.6.1	Spatial Resolution	3
1.6.2	Projection and Grid Description	3
1.7	Temporal Coverage.....	3
1.7.1	Temporal Resolution.....	3
1.8	Parameter or Variable	3
1.8.1	Parameter Description	3
1.8.2	Sample Data Record.....	4
2	SOFTWARE AND TOOLS	4
2.1	Get Data	4
2.2	Software and Tools.....	4
2.3	Quality Assessment.....	4
3	DATA ACQUISITION AND PROCESSING.....	4
3.1	Theory of Measurements.....	4
3.2	Data Acquisition Methods.....	4
3.3	Derivation Techniques and Algorithms.....	4
3.3.1	Trajectory and Attitude Data	5
3.3.2	Processing Steps	5
3.3.3	Version History.....	5
3.3.4	Errors and Limitations	5
4	REFERENCES AND RELATED PUBLICATIONS	5
4.1	Related Data Collections.....	5
4.2	Related Websites	5
5	DOCUMENT INFORMATION.....	5
5.1	Publication Date	5
5.2	Date Last Updated.....	5
6	APPENDICES.....	6
6.1	Appendix A -	6
6.2	Appendix B -	6

1 DETAILED DATA DESCRIPTION

The data set includes measurements for echograms, time, latitude, longitude, and elevation, as well as flight path charts and echogram images.

Operation IceBridge products may include test flight data that are not useful for research and scientific analysis. Test flights usually occur at the beginning of campaigns. Users should read flight reports for the flights that collected any of the data they intend to use. Check IceBridge campaign Flight Reports for dates and information about test flights.

1.1 Format

The data files are in MATLAB Version 6 numerical computing files. Additional associated files are provided in PNG, JPEG, KML, and PDF formats.

The radar data are divided into segments. A segment is a contiguous data set in which the radar settings do not change. A day is divided into segments if the radar settings were changed, hard drives were switched, or other operational constraints required that the radar recording be turned off and on. The segment ID is YYYYMMDD_SS where YYYY is the four-digit year (e.g. 2011), MM is the two-digit month from 1 to 12, DD is the two-digit day of the month from 1 to 31, and SS is the segment number from 0 to 99. Segments are always sorted in the order in which the data was collected. Generally SS starts with 1 and increments by 1 for each new segment, but this is not always the case; only the ordering is guaranteed to match the order of data collection.

Each segment is broken into frames, analogous to satellite SAR scenes, to make analyzing the data easier. Most frames are 50 km long, but some may be longer or shorter so the breaks between frames lie at convenient locations. For example, if a grid is flown, the frames are aligned from adjacent lines. Once the frame boundaries are defined, they will not change from one release to the next or one processing method to the next. The frame ID is a concatenation of the segment ID and a frame number and follows the format YYYYMMDD_SS_FFF where FFF is the frame number from 000 to 999. Generally the FFF starts with 0 or 1 and increments by 1 for each new frame, but this is not always the case; only the ordering is guaranteed.

Frames may overlap slightly so data are duplicated where the overlap occurs. GPS time can be used to remove redundant data from the overlapped sections.

For each data frame there may be many different L1B products depending on how waveforms and channels are combined and how the processing is done (see Data Processing section). For each data frame there is a flight path file (0map), an echogram file (1echo), and an echogram overlaid with surface and bottom picks (2echo_picks).

1.2 File and Directory Structure

Data are available on the following HTTPS site:

https://daacdata.apps.nsidc.org/pub/DATASETS/ICEBRIDGE/IRMCR1B_MCORDSxyEcho_v01/

Within this directory, the folders are organized by date, and containing subdirectories as listed below:

```
/2009_AN_CREISIS/  
/2009_AN_NASA/  
/2010_AN_NASA/  
/2010_GR_NASA/  
/2012_2011_AN_NASA/  
/2011_2011_GR_NASA/  
/2013_2012_AN_NASA/  
/2012_2012_GR_NASA/  
/CSARP_standard/  
    /images/  
    /kml/  
    /pdf/
```

1.2.1 Sub-Directory Folders

`/CSARP_standard/`

Standard Synthetic Aperture Radar (SAR) processed output. The receiver-array elements are combined using boxcar or Hanning weights, depending on the frame. Files in the `/images/` and `/pdf/` directories are derivatives for viewing. The most convenient way to browse the imagery quickly is through the PDF files in the `/pdf/` directory.

`/images/`

All of the PNG or JPEG files are in this directory. This includes for each frame a flight path file, an echogram file, and an echogram overlaid with surface and bottom picks. The background images are Landsat-7 natural color imagery in polar stereographic format. Center for Greenland/Canada is

70 degrees true scale latitude, -45 degrees longitude. Center for Antarctica is -71 degrees true scale latitude, 0 degrees longitude.

/km1/

Flight lines for each segment.

/pdf/

Same images as the PNG and JPEG files, except all images from a segment are concatenated into a single PDF file for convenient browsing.

1.3 File Naming Convention

1.3.1 MATLAB Files

The data files have the naming conventions shown below and as described in Table 1.

Data_20091016_01_001.mat

Data_YYYYMMDD_SS_FFF.mat

Where:

Table 1. MATLAB File Naming Convention

Variable	Description
Data	MCoRDS data
YYYY	4-digit year
MM	2-digit month
DD	2-digit day
SS	day segment
FFF	frame number
.mat	indicates a MATLAB file

1.3.2 PNG and JPEG Image Files

The PNG and JPEG image files have the naming conventions shown below and as described in Table 2.

NOTE: From 2009 through 2011, images files in the /images/ folders are PNG files. Starting in 2012 the image files are JPEG files.

20101104_06_001_163923_0maps.png
 20101104_06_001_163923_1echo.png
 20101104_06_001_163923_2echo_picks.png

YYYYMMDD_SS_FFF_HHmms_0maps.nnn
 YYYYMMDD_SS_FFF_HHmms_1echo.nnn
 YYYYMMDD_SS_FFF_HHmms_2echo_picks.nnn

Where:

Table 2. PNG and JPEG Image File Naming Convention

Variable	Description
YYYY	4-digit year
MM	2-digit month
DD	2-digit day
SS	segment number
FFF	frame number
HH	GPS time stamp hour for the first range line in the image, 00-23
mm	GPS time stamp minute for the first range line in the image, 00-59
ss	GPS time stamp second for the first range line in the image, 00-59
0maps	flight path file
1echo	echogram file
2echo_picks	echogram overlaid with surface and bottom picks
.nnn	image file type .png = PNG file .jpg = JPEG file

1.3.3 KML Image Files

The KML files have the naming conventions shown below and as described in Table 3.

Browse_2009_Antarctica_DC8.kml
 Browse_Data_20091016_01.kml

Browse_YYYY_location_nnn.kml
 Browse_Data_YYYYMMDD_SS.kml

Where:

Table 3. KML File Naming Convention

Variable	Description
Browse or Browse_Data	browse file
YYYY	4-digit year
location	Antarctica or Greenland
nnn	aircraft identifier, DC-8 or P-3
MM	2-digit month
DD	2-digit day
SS	segment number
.kml	indicates KML file

1.3.4 PDF Files

The PDF files have the naming conventions shown below and as described in Table 4.

20091016_01.pdf

YYYYMMDD_SS.pdf

Where:

Table 4. PDF File Naming Convention

Variable	Description
YYYY	4-digit year
MM	2-digit month
DD	2-digit day
SS	segment number
.pdf	indicates PDF file

1.4 File Size

MATLAB files range from approximately 384 KB to 73 MB.

PNG files range from approximately 40 KB to 1 MB.

JPEG files range from approximately 54 KB to 193 KB.

KML files range from approximately 6 KB to 9.5 MB.

PDF files range from approximately 3 KB to 40 MB.

1.5 Volume

The entire data set is approximately 164 GB.

1.6 Spatial Coverage

Spatial coverage for this data set includes Antarctica and Greenland.

Antarctic:

Southernmost Latitude: 90° S

Northernmost Latitude: 63° S

Westernmost Longitude: 180° W

Easternmost Longitude: 180° E

Greenland:

Southernmost Latitude: 59° N

Northernmost Latitude: 83° N

Westernmost Longitude: 74° W

Easternmost Longitude: 12° W

1.6.1 Spatial Resolution

Spatial resolution varies depending on the platform and year. See the Derivation Techniques and Algorithms section for further detail on resolution and bandwidth. An example is given here for the 2010 Antarctica DC-8 mission.

Smooth surface, across-track:

641 m resolution for aircraft height = 500 m and ice thickness = 2000 m.

1518 m resolution for aircraft height = 8000 m and ice thickness = 2000 m.

The band ranges from 189.15 MHz to 198.65 MHz. The width of the band is 9.5 MHz.

Rough surface, across-track:

965 m resolution for aircraft height = 500 m and ice thickness = 2000 m.

5416 m resolution for aircraft height = 8000 m and ice thickness = 2000 m.

Antenna array beamwidth $\beta = 34\text{deg} \cdot \pi / 180\text{deg}$ (radians).

Along-track resolution depends on processing. See Derivation Techniques and Algorithms for details.

Depth Resolution: 13.6 m.

1.6.2 Projection and Grid Description

These data are provided in WGS-84 geodetic coordinates and WGS-84 ellipsoid elevation reference. Image files are in Operation IceBridge polar stereographic projections for Greenland Standard Parallel 70° N and Longitude of the Origin 45° W, and Antarctica Standard Parallel 71° S and Longitude of the Origin 0° E.

1.7 Temporal Coverage

16 October 2009 to 17 May 2012

1.7.1 Temporal Resolution

IceBridge campaigns are conducted on an annually repeating basis. Arctic and Greenland campaigns are conducted during March, April, and May; Antarctic campaigns are conducted during October and November.

1.8 Parameter or Variable

This data set contains measurements for elevation, surface, and bottom.

1.8.1 Parameter Description

The MATLAB files contain fields as described in Table 5.

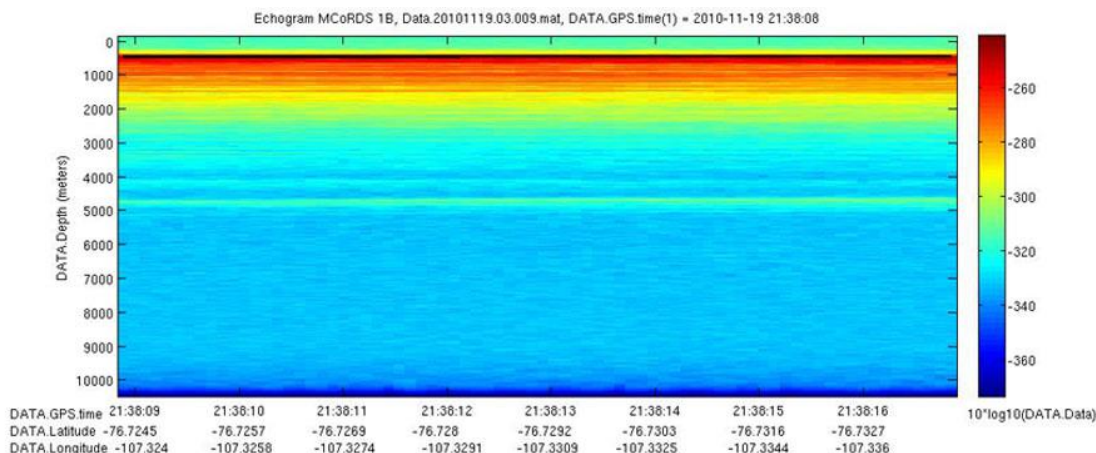
Table 5. MATLAB File Parameters, Description, and Units

Parameter	Description	Units
Data	Radar echogram data.	Relative received power (Watts)
Time	Fast time. Zero time is the beginning of the transmit event calibrated to within one range resolution cell.	Seconds
Depth	Range axis assuming a vacuum media ($Depth = Time * c/2$).	Meters
GPS_time	GPS time when data were collected. Seconds since 01 January 1970 00:00:00. The ANSI C standard.	Seconds
Latitude	WGS-84 geodetic latitude coordinate. Always referenced to North. Represents the location of the radar echogram data phase center. May not be the actual measurement location due to motion compensation.	Degrees

Parameter	Description	Units
Longitude	WGS-84 geodetic longitude coordinate. Always referenced to East. Represents the location of the radar echogram data phase center. May not be the actual measurement location due to motion compensation.	Degrees
Elevation	Referenced to WGS-84 ellipsoid. Positive is outward from the center of the Earth. Without motion compensation, represents the location that the trajectory data was processed to. With motion compensation, represents the location of the radar echogram data phase center. It may not be the actual measurement location due to motion compensation.	Meters
Surface	Estimated two way propagation time to the ice surface from the phase center. Uses the same frame of reference as the Time variable. This information is used during SAR processing to determine where the dielectric half-space between air and ice should be. This is not the L2 product although they are often the same.	Seconds
Bottom	Estimated two way propagation time to the ice bottom from the phase center. This uses the same frame of reference as the Time variable. This information is used during 3D-imaging to determine where the ice bed may be. This is not the MCoRDS Level-2 product although they are often the same.	Seconds
param	Multiple variables with a name containing the string "param". Contains 1) Radar and processing settings, 2) Processing software version and time stamp information. Fields of structures are not static and may change from one version to the next.	N/A

1.8.2 Sample Data Record

Shown below is an image of the data values from the MCoRDS Level-1B 2010 Antarctica file Data_20101119_03_009.mat. This image depicts all parameters except Time, which is better explained as $\text{Time} \times \text{speed-of-light-through-medium} / 2 = \text{Depth}$.



Data_20101119_03_009.mat contains DATA complete raw values:

DATA: =

Bottom: [1x76 double] (NaN's for this data)

Data: [673x76 double] (magnitude) image

Depth: [1x673 double] (meters) y-axis

Elevation: [1x76 double] (meters) x-axis

GPS_time: [1x76 double] (seconds since 1970 Jan,1,00:00) x-axis

Latitude: [1x76 double] (dec.deg.) x-axis

Longitude: [1x76 double] (dec.deg) x-axis

Surface: [1x76 double] (seconds) Plotted in a black line near 0 meters Depth

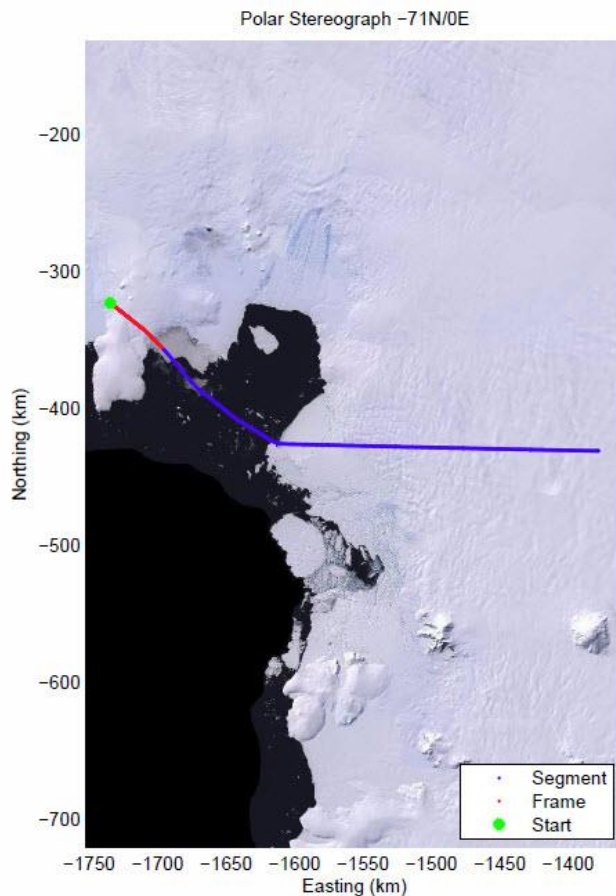
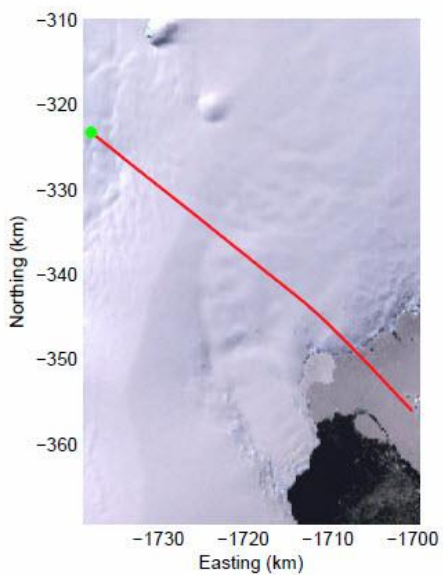
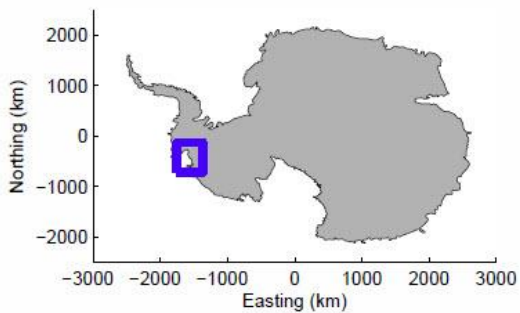
Time: [1x673 double] (seconds) $Time * c / 2 = Depth$

array_param: [1x1 struct]

param_csarp: [1x1 struct]

param_radar: [1x1 struct]

The image below shows the content of the 20101119_03.pdf file that corresponds with the Data_20101119_03_009.mat data file illustrated above.



2 SOFTWARE AND TOOLS

2.1 Software and Tools

The MATLAB files may be opened using MATLAB, or using an open source tool such as Octave. [C and IDL readers](#) for MATLAB files are also available on the NSIDC FTP site.

The PNG files may be opened using any program capable of reading Portable Network Graphics files.

The JPEG files may be opened using any program capable of reading Joint Photographic Experts Group files.

The PDF files may be opened using any program capable of viewing Portable Document Format files.

KML files are read by GIS software packages and earth browsers such as Google Earth or Google Maps.

2.2 Quality Assessment

The high altitude data are generally lower quality than the low altitude data. This is because:

1. The cross-track antenna resolution is proportional to range creating severe layover problems in mountainous terrain, for example 05 November 2009 high altitude peninsula flight.
2. The sidelobes from the 30 microsecond pulse duration mask out some of the returns that otherwise would have had a high enough signal to noise ratio.
3. The range to target is greater so the spherical spreading power loss is greater leading to a lower signal to noise ratio.

3 DATA ACQUISITION AND PROCESSING

For the standard processing output, the receiver-array elements are combined using boxcar or Hanning weights, depending on the frame.

Some of the results are processed through an improved array processing algorithm. The receiver-array elements are combined using the minimum variance distortionless response algorithm which provides improved cross-track clutter rejection. Cross-track clutter rejection is important because the footprint of the antenna array is very large in the cross-track dimension.

3.1 Theory of Measurements

When a pulse of RF energy is transmitted into the ice sheet, a portion of the energy is reflected from the ice surface, ice bottom, and any englacial targets; generally anywhere there is a contrast in the electromagnetic constitutive properties of the media. To detect the ice bottom, lower frequencies are used because they do not attenuate as quickly through ice (Paden, 2005).

Ice thickness is typically determined using data collected from waveforms with different pulse durations. Generally all receive channels are used to produce the best result. The difference in the propagation time between the ice surface and ice bottom reflections is then converted into ice thickness using an estimated ice index of refraction of ice (square root of 3.15). The media is assumed to be uniform, that is, no firm correction is applied. The specific measurement setups for four data collection modes are described in the Data Acquisition section for the four different data collection scenarios. See also the related MCoRDS Level 2 data documentation, IceBridge MCoRDS L2 Ice Thickness.

3.1.1 Dynamic Range

The signal from the ice surface is typically much larger than the signal from the ice bottom. This is because of the attenuation of RF signals in ice. Generally speaking this requires that different receiver gains are used to capture these signals. Three methods have been used by the radar systems.

The sensitivity timing control (STC) is a fast-time gain control where the receiver gain is modified in real-time as the echoes are received. The original sensitivity timing control used a hand dial to control the STC and the STC was analog (not discrete). Radiometric calibration of the data is nearly impossible with these datasets.

Low and high gain channels means that two separate recordings of the data are made: one with low receiver gain and one with high receiver gain. It provides the most flexible and best quality dynamic range, but generally doubles the data rate and much of the hardware must be duplicated to capture two channels.

A waveform playlist allows low and high gain channels to be multiplexed in time. The low gain channel typically requires fewer integrations to be useful and so only a small penalty is paid for time multiplexing. If time was split equally it would be 3 dB, but typical configurations lose less than 1 dB of sensitivity. Alternatively, two waveforms, one with a short pulse duration and one with a long pulse duration, generally provide better coverage than a single pulse duration. The short pulse duration is used for close-in targets that typically do not require high sensitivity and so this waveform doubles as the low gain channel and effectively no penalty is paid for time multiplexing

the gain settings. For example, a waveform with a 1- μ s duration and lower receiver gain settings is used to measure the round-trip signal time for the ice surface echo, while a waveform with a 10- μ s duration and higher receiver gain settings is used to measure the round-trip signal time for the ice bottom echo. As stated above, the two different waveforms are used because of the large dynamic range of signal powers that are observed. The 10- μ s duration and higher receiver gain settings are more sensitive to the bottom echo, but the signal is generally saturated and unusable from the ice surface and upper internal layers.

For high altitude data, the difference in power between the ice surface and ice bottom is small enough that a single high gain setting is possible.

3.2 Data Acquisition Methods

3.2.1 P-3 Low Altitude

A waveform with a 1- μ s duration and lower receiver gain settings is used to measure the round-trip signal time for the surface echo, while a waveform with a 10- μ s duration and higher receiver gain settings is used to measure the round-trip signal time for the bed echo. The two different waveforms are used because of the large dynamic range of signal powers that are observed. The 10- μ s duration and higher receiver gain settings are more sensitive to the bed echo, but the signal is generally saturated from the ice surface and upper internal layers.

3.2.2 DC-8 Low Altitude

The same concept is used as for the P-3. However, during the first two field seasons (2009 Antarctica DC-8 and 2010 Greenland DC-8), extra antennas inside the cabin were used to detect the ice surface delay time because the Transmit/Receive (TR) switches did not meet their switching time specification. The TR switches have not been fixed in subsequent field seasons, but the TR switch control signals have been set so that the surface echo is generally still detectable, although with diminished power, even for very low altitudes down to 600 feet Above Ground Level (AGL).

3.2.3 P-3 High Altitude and DC-8 High Altitude

The dynamic range between the ice surface and ice bottom echoes is much smaller and a single high-gain and long pulse duration waveform is used to capture both echoes.

2009 Antarctica DC-8 Radar Settings

Bandwidth: 180-210 MHz (DC-8 platform restricted to 189.15-198.65 MHz)

Tx power: 550 W

Waveform: eight channel chirp generation, 14 bit ADC at 111 MHz bandpass sampling

Acquisition: eight channels
Dynamic Range: waveform playlist
Rx Aperture: 1.5 wavelength aperture
Tx Aperture: 1.5 wavelength aperture; fully programmable
Monostatic Rx/Tx
Data rate: 12 MB/sec per channel

2009 Antarctica Twin Otter Radar Settings

Bandwidth: 140-160 MHz
Tx power: 500 W
Waveform: eight channel chirp generation
Acquisition: eight channels
Rx Aperture: 3 wavelength aperture
Tx Aperture: 3 wavelength aperture; fully programmable
Bistatic Rx/Tx
Data rate: 12 MB/sec per channel

2010 Antarctica DC-8 Radar Settings

Dynamic Range: waveform playlist coupled with low gain and high gain channels

2010 Greenland P-3 Radar Settings

Bandwidth: 180-210 MHz (EMI restricted to 10 MHz within 180-210 MHz most segments)
Tx power: 600 W
Waveform: eight channel chirp generation
Acquisition: sixteen channels (multiplexed on to 8 channels), 14 bit ADC at 111 MHz bandpass sampling
Rx Aperture: 2 wavelength, 3.5 wavelength, and 2 wavelength apertures, baseline of 6.4 m between each aperture
Tx Aperture: 3.5 wavelength aperture; fully programmable
Mixed monostatic and bistatic tx/rx
Data rate: 6 MB/sec per channel

2011 Antarctica DC-8 Radar Settings

Dynamic Range: waveform playlist coupled with low gain and high gain channels

2011 Antarctica Twin Otter Radar Settings

Tx power: 1500 W
Rx Aperture: two 3 wavelength apertures with 13.8 m baseline
Tx Aperture: 3 wavelength aperture; fully programmable

2011 Greenland Twin Otter Radar Settings

Bandwidth: 180-210 MHz

Tx power: 500 W

Waveform: eight channel chirp generation

Acquisition: sixteen channels (multiplexed onto 8 channels), 14 bit ADC at 111 MHz bandpass sampling

Rx Aperture: two 3 wavelength apertures with 13.8 m baseline

Tx Aperture: 3 wavelength aperture; fully programmable

Mixed monostatic and bistatic tx/rx

Data rate: 6 MB/sec per channel

2011 Greenland P-3 Radar Settings

Bandwidth: 180-210 MHz

Tx power: 1050 W

Waveform: Eight channel chirp generation

Acquisition: sixteen channels, 14 bit ADC at 111 MHz bandpass sampling

Dynamic Range: waveform playlist

Rx Aperture: 2 wavelength, 3.5 wavelength, and 2 wavelength apertures, baseline of 6.4 m between each aperture

Tx Aperture: 3.5 wavelength aperture; fully programmable

Mixed monostatic and bistatic tx/rx

Data rate: 32 MB/sec per channel

3.3 Derivation Techniques and Algorithms

3.3.1 Range Resolution

The range resolution, defined as the minimum range difference to distinguish the return power from two targets with 16 dB of isolation, is determined as:

$$\frac{K_t c}{2B \sqrt{\epsilon_{r,ice}}} \quad (\text{Equation 1})$$

Where:

Table 6. Flat Surface Depth Resolution

Variable	Description
k_t	window widening factor. 0.88 for no windowing and 1.53 for 20% Tukey time-domain window on transmit and receive and a Hanning frequency-domain window on receive.
c	speed of light in a vacuum
B	bandwidth
$\epsilon_{r,ice}$	3.15, the approximate dielectric of ice

The window widening factor is computed numerically. Windowing is applied to improve the isolation between targets at different ranges, but causes the resolution to become worse.

Table 7 gives the range resolution for several bandwidths.

Table 7. Range Resolution

Bandwidth (MHz)	Range Resolution without windowing (m)	Range Resolution with windowing (m)
9.5	7.8	13.6
10	7.4	12.9
17.5	4.2	7.4
20	3.7	6.5
30	2.5	4.3
150	0.5	0.9
180	0.4	0.7

If there is only one target, the range accuracy to that one target is dependent on the Signal to Noise Ratio (SNR), and is given by:

$$\frac{K_t c}{2B \sqrt{\epsilon_{r,ice}} \sqrt{2 \cdot \text{SNR}}} \quad (\text{Equation 2})$$

Table 8 repeats Table 7 with SNR of 20 dB.

Table 8. Range Resolution - One Target

Bandwidth (MHz)	Range Resolution without windowing (m)	Range Resolution with windowing (m)
9.5	0.55	0.96
10	0.53	0.91
17.5	0.30	0.52

Bandwidth (MHz)	Range Resolution without windowing (m)	Range Resolution with windowing (m)
20	0.26	0.46
30	0.18	0.30
150	0.04	0.06
180	0.03	0.05

3.3.2 Along-track Resolution

The along-track resolution depends on the processing. The default processing parameters since March 1, 2012 are described here. For the single look complex (SLC) SAR-processed image (not quick look), a fixed along-track resolution of $\sigma_{x,SLC} = 5$ m is used. The final product has 11 along-track looks and 1 range look and is then decimated by 6. Therefore, the final product has an along-track resolution of $\sigma_x = 55$ m and a sample spacing of 30 m. The synthetic aperture length, L , is approximately:

$$L \approx \frac{\lambda_c \left(H + T / \sqrt{\epsilon_{r,ice}} \right)}{2\sigma_{x,SLC}} K_x \quad \text{(Equation 3)}$$

Where:

Table 9. Synthetic Aperture Length

Variable	Description
λ_c	wavelength at the center frequency
H	height above the air/ice interface
T	ice thickness
$\epsilon_{r,ice}$	3.15, the approximate dielectric of ice
K_x	1.1, the along-track windowing factor for a 20% tukey window
$\sigma_{x,SLC}$	5 m fixed along track resolution

The Doppler beam width, β_x , used in the SAR processing is approximately:

$$\beta_x \approx \frac{\lambda_c}{2\sigma_{x,SLC}} K_x = 9.7 \text{ deg} \quad \text{(Equation 4)}$$

3.3.3 Cross-track Resolution

While the range and along-track position are known with fine resolution, the cross-track resolution is poor. For a rough surface, the off-nadir echoes can mask the nadir echo and an off-nadir return may be selected as the ice bottom rather than the nadir return. The best case is to have crossovers in the dataset so you can estimate the precision of the ice bottom layer picks.

For a smooth surface with no appreciable roughness, the cross-track resolution is constrained to the first Fresnel zone, which is approximately:

$$\sigma_{y, \text{Fresnel-limited}} = \sqrt{2 \left(H + T / \sqrt{\epsilon_{r, \text{ice}}} \right) \lambda_c} \quad \text{(Equation 5)}$$

Where:

Table 10. Smooth Surface Cross-track Resolution

Variable	Description
H	height above the air/ice interface
T	ice thickness
$\epsilon_{r, \text{ice}}$	3.15, the approximate dielectric of ice
λ_c	wavelength at the center frequency

Table 11 gives the cross-track resolution for several frequencies.

Table 11. Cross-track Resolution

Center Frequency (MHz)	Cross-track Resolution H = 500 m T = 2000 m (m)	Cross-track Resolution H = 8000 m T = 2000 m (m)
125	88.3	209.2
150	80.6	191.0
195	70.7	167.5
210	68.2	161.4

For a rough surface with no appreciable layover, the cross-track resolution is constrained by the pulse-limited footprint, which is approximately:

$$\sigma_{y, \text{pulse-limited}} = 2 \sqrt{\frac{\left(H + T / \sqrt{\epsilon_{r, \text{ice}}} \right) c K_t}{B}} \quad \text{(Equation 6)}$$

Where:

Table 12. Rough Surface Cross-track Resolution

Variable	Description
H	height above the air/ice interface
T	ice thickness
$\epsilon_{r,ice}$	3.15, the approximate dielectric of ice
c	speed of light in a vacuum
Kt	window widening factor
B	bandwidth

Table 13 gives the cross-track resolution with windowing.

Table 13. Cross-track Resolution with Windowing

Bandwidth (MHz)	Cross-track Resolution H = 500 m T = 2000 m (m)	Cross-track Resolution H = 500 m T = 8000 m (m)
9.5	561	1328
10	546	1294
17.5	413	978
20	386	915
30	315	747
150	141	334
180	129	305

For a rough surface where layover occurs, the cross-track resolution is set by the beamwidth β_y of the antenna array. The antenna beamwidth is approximately:

$$\beta_y = \sin^{-1} \frac{\lambda_c}{Nd_y} \text{ (Equation 7)}$$

Where:

Table 14. Rough Surface with Layover Cross-track Resolution

Variable	Description
B_y	beamwidth of antenna array
λ_c	wavelength at the center frequency
N	number of elements
d_y	element spacing

Table 15 gives the beamwidth for the various platforms.

Table 15. Beamwidth for Various Platforms

Platform	N	d _y (λ _c)	Beamwidth (deg)
P-3 original	4	0.5	30.0
TO	4	0.5	30.0
TO	5	0.5	23.6
TO	6	0.5	19.5
P-3 new (center-array only)	7	0.5	16.6
DC-8	5	0.25	53.1

3.3.4 Antenna Beamwidth

The antenna beamwidth-limited resolution is:

$$\sigma_{y, \text{beamwidth-limited}} = 2 \left(H + \frac{T}{\sqrt{\epsilon_{r, \text{ice}}}} \right) \tan \left(\frac{\beta_y K_y}{2} \right) \quad \text{(Equation 8)}$$

Where:

Table 16. Antenna Beamwidth-limited Resolution

Variable	Description
H	height above the air/ice interface
T	ice thickness
ε _{r,ice}	3.15, the approximate dielectric of ice
β _y	beamwidth of antenna array in radians
K _y	K _y = 1.3, the approximate cross-track windowing factor for a Hanning window applied to a small cross-track antenna array.

Examples of antenna beamwidth-limited resolution are shown in Table 17.

Table 17. Antenna Beamwidth-limited Resolution

Platform	N	d _y (λ _c)	Cross-track Resolution H = 500 m T = 2000 m	Cross-track Resolution H = 500 m T = 8000 m
P-3 original	4	0.5	1152	3546
TO	4	0.5	1152	3546
TO	5	0.5	893	2747
TO	6	0.5	732	2252

Platform	N	d_y (λ_c)	Cross-track Resolution H = 500 m T = 2000 m	Cross-track Resolution H = 500 m T = 8000 m
P-3 new (center-array only)	7	0.5	620	1909
DC-8	5	0.25	2237	6887

3.3.5 Dielectric Error

The dielectric error is expected to be on the order of one percent for typical dry ice (Fujita et al., 2000) and no compensation has been done for a firn layer in SAR processing where the ice is treated as a homogeneous medium with a dielectric of 3.15. The dielectric error using the first term of the Taylor series creates an ice thickness dependent error given by:

$$\Delta T = \frac{-T}{2} \varepsilon_{\%error} = \frac{-T}{200} \text{ (Equation 9)}$$

So for an ice thickness of T = 2000, a one percent dielectric error creates a 10 m thickness error.

3.3.6 System Loop Sensitivity

The system loop sensitivity is the SNR with no channel losses (spreading loss, extinction, and backscattering), which is:

$$SNR = \frac{P_t (N_c G \lambda_c)^2 N_{ave} B T_{pd}}{4\pi k T B F \cdot m^2} \text{ (Equation 10)}$$

Where:

Table 18. System Loop Sensitivity

Variable	Description
P_t	total transmit power including system losses
N_c	number of channels on transmit and receive used in echogram formation
G	individual antenna element accounting for the ground plane
λ_c	wavelength at the center frequency in air
N_{ave}	approximate number of pulses that may be averaged in SAR processing and presumming
B	bandwidth
T_{pd}	pulse duration
k	$1.38e-23 \text{ W s K}^{-1}$, Boltzmann's constant

Variable	Description
T	290 K, the approximated noise temperature before the receiver
F	2, the approximate noise figure of the receiver
m^2	1 meter squared to cancel out units

System loop sensitivity values are shown in Table 19.

Table 19. Loop Sensitivity Values

Platform	P_t	N_c	G	N_{ave}	T_{pd} ($\hat{A}\mu s$)	$\lambda_c(m)$	Loop Sensitivity (dB)
MCORDS DC-8	300	5	1	3200	10	1.54	220
MCORDS P-3	166	7	4	3200	10	1.54	230
MCORDS Twin Otter (150 MHz)	300	6	4	3200	10	2	233
MCRDS TO	300	6	4	3200	10	1.54	231

3.3.7 Processing Steps

The following processing steps are performed by the data provider.

1. Conversion from quantization to voltage at the 50 ohm antenna.
2. Removal of DC-bias by subtracting the mean from each record.
3. Channel compensation between each of the antenna phase centers. This includes time delay, amplitude, and phase mismatches. The channel equalization coefficients are found by monitoring the relative returns from each channel from the ocean surface at high altitude, smooth bed returns, and deep internal layers.
4. Pulse compression with time and frequency domain windows. Before the 2009 Antarctica DC-8 campaign, the transmitted pulse had a boxcar window. From 2009 Antarctica DC-8 and forward, all transmitted pulses typically have a 20 percent Tukey window applied in the time domain. The matched filter applied to the received signal is identical to the transmitted waveform, typically assuming an ideal transmission, with a frequency domain window applied. The frequency domain window is usually a boxcar or Hanning window.
5. Motion compensation for attitude and trajectory lever arm.
6. SAR processing with along-track spatial frequency window using f-k migration. The dielectric model for f-k migration is always a layered media with variation in the z-axis only.
7. Channel combination. Currently, channel combination usually combines channels within a sub-array. Standard SAR processed output applies a normalized array window before summing channels. Minimum Variance Distortionless Response (MVDR) algorithm is used for channel combination, and the spatial correlation matrix is estimated from a neighborhood of pixels surrounding the image pixel being combined. Channel combination also includes multi-looking or spatial incoherent power averaging followed by along-track decimation.
8. Waveform combination. Echograms from low and high gain channels are combined to form a single image. Generally combination is done T_{pd} seconds after the surface return where T_{pd} is the pulse duration of the transmitted chirp.

3.3.8 Version History

On April 12, 2011, 2009 Antarctica MCoRDS data were replaced by V01.1. The original 2009 Antarctica data were processed through a temporary process with quick look data products only. V01.1 data are produced from full SAR processing.

On May 16, 2011, the 2010 Antarctica MCoRDS data were replaced by V01.2. The initial 2010 Antarctica data release was a quick look product released immediately upon return from the field. It was Synthetic Aperture Radar (SAR) processed, but the cross-track array processing was greatly simplified. The V01.2 release is the standard product produced from full SAR processing.

On 17 October 2011, the V01.2 MCoRDS data were replaced by V01.3. In V1.03, the `kml_good` directories have been removed. The echogram data product offerings have been trimmed to a single echogram per data nodule. V1.02 included `CSARP_csarp-combined`, `CSARP_standard`, `CSARP_mvdr`, and `CSARP_qlook`. V1.03 includes only `CSARP_standard`. All "`Data_img_01_YYYY...`" and "`Data_img_02_YYYY...`" files have been removed so that the only files left are the "`Data_YYYY...`" files. In the case where only a single image file was produced in the past, i.e. "`Data_img_01_YYYY...`" these have been renamed to "`Data_YYYY...`".

On 13 November 2012, the 2012 Greenland data were replaced with Version 01.4. The IRMCR1B results have one data segment added and one removed from the original data posting of 26 July 2012.

On 16 November 2012, the 2012 Greenland data were replaced with Version 01.4. One data segment was added and one segment was removed from the original 2012 Greenland data posted in July 2012. All of the 2012 Greenland data have been reprocessed but the difference in content between Version 01.3 and 01.4 should be negligible. If you downloaded the 2012 Greenland data prior to November 16, 2012, it is recommended to re-download the data.

Version 2 IRMCR1B data: beginning with the 2012 Antarctica campaign, all data are provided in netCDF format. In the near future, all Version 1 data will be replaced with netCDF data. For more on Version 2 IRMCR1B data see the Version 2 documentation.

3.3.9 Error Sources

The data are not radiometrically calibrated. This means that they are not converted to some absolute standard for reflectivity or backscattering analysis. The MCoRDS science team is working on data processing and hardware modifications to do this.

The primary error sources for ice penetrating radar data are system electronic noise, multiple reflectors also known as multiples, and off-nadir reflections. Each of these error sources can create

spurious reflections in the trace data leading to false echo layers in profile data. Multiple reflectors arise when the radar energy reflects off three surfaces back-and-forth in the vertical dimension, and then returns to the receive antenna. They occur in situations when multiple surfaces are present with high impedance, such as the upper surface (air/ground), the base of the ice or an ice-water interface, and the aircraft body which is also a strong reflector. The radar receiver only records time since the radar pulse was emitted, so the radar energy that traveled the additional path length appears later in time, apparently deeper in the ice or even below the ice-bedrock interface. Note that multiples of a strong continuous reflector have a similar shape but all slopes appear magnified, that is, doubled in the simplest geometric cases, relative to the main reflection.

Off-nadir reflections can result from crevasse surfaces, water, rock outcrops, or metal structures. Antenna beam structure and processing of the MCoRDS system are designed to reduce these off-nadir reflected energy sources.

For Standard processing output from waveform 1 only, for thin ice, the longer pulse duration of the high gain waveform may mean that sidelobes from the surface echo mask the bottom return. In these cases, waveform 2, with short pulse duration, can provide a better measurement.

A time stamp error was discovered in the 2012 Antarctica data originally published in .mat files. The latest leap second (July 1, 2012) was not accounted for in the GPS times for these campaigns. This error has been corrected in the 2012 Antarctica data that are now included in IRMCR1B V2 netCDF format.

2009 Antarctica DC-8 Specific Issues

Transmit/Receive Switch: During the first two field seasons (2009 Antarctica DC-8 and 2010 Greenland DC-8), extra antennas inside the cabin were used to detect the ice surface delay time because the TR switches did not meet their switching time specification. The TR switches have not been fixed in subsequent field seasons, but the TR switch control signals have been set so that the surface echo is generally still detectable, although with diminished power, even for very low altitudes down to 600 ft. AGL.

Some of the data collected during this season are from high altitude. The high altitude data are generally lower quality than the low altitude data. This is because:

the cross-track antenna resolution is proportional to range creating severe layover problems in mountainous terrain, for example 05 November 2009 high altitude peninsula flight.

the sidelobes from the long pulse duration mask out some of the returns that otherwise would have had a high enough signal to noise ratio.

the range to target is greater so the spherical spreading power loss is greater leading to a lower signal to noise ratio.

Monostatic elements: All monostatic elements used for transmit and receive have an unknown fast-time gain profile because the transmit/receive switches take about 10 microseconds to fully switch positions. This fast-time gain profile has not been corrected so that using the surface or shallow layer returns for antenna equalization or for radiometric purposes is not recommended. All five of the antennas on the DC-8 are monostatic antennas.

2010 Antarctica DC-8 Specific Issues

Transmit/Receive Switch: This is a similar problem as with the 2009 Antarctica DC-8 season. However, we were able to set the TR switch control signals so that the surface is recoverable with the regular array down to an altitude of 600 ft. AGL but with very much reduced signal strength. The regular array is preferred over the EMI antenna setup because the radiation pattern characteristics are better. At an altitude of 1500 ft., no degradation in signal detectability is observed.

High altitude data: See 2009 Antarctica DC-8.

Monostatic elements: See 2009 Antarctica DC-8.

2010 Greenland DC-8 Specific Issues

One of the in-cabin Electromagnetic Interference (EMI) antennas is used to produce the quick look data product. The EMI antennas were not designed to receive the surface return. However, the transmit-receive switch for the primary array was set so that the surface returns for platform altitudes below 1500 feet were greatly attenuated. Because of this, the EMI antennas are used for picking the surface return at low altitude.

2010 Greenland P-3 Specific Issues

Monostatic elements: See 2009 Antarctica DC-8. Only the center seven elements are monostatic on the P-3.

EMI: Due to lack of shielding, a noisy switching power supply, and potentially other unidentified sources the radar was operated with 10 MHz bandwidth (190-200 MHz) for most of the field season. The signal quality is still lower than expected in this band due to broadband noise which is present at all times and periodic burst noise from other pulsed instruments on the P-3 and from random burst noise. The noise present at all times manifests itself as an increase in the noise floor and the burst noise manifests itself as smeared point targets.

2011 Greenland P-3 Specific Issues

The MCoRDS2 data acquisition system fielded for the first time this season has a known issue with radar data synchronization with GPS data. The synchronization time correction that must be added to the radar time stamp is either 0 or -1 second. When the radar system is initially turned on, the radar system acquires Universal Time Coordinated (UTC) time from the GPS National Marine Electronics Association (NMEA) string. If this is done too soon after the GPS receiver has been turned on, the NMEA string sometimes returns GPS time rather than UTC time. GPS time is 15 seconds ahead of UTC time during this field season. The corrections for the entire day must include the offset, either -15 or -16 seconds. GPS corrections have been applied to all of the data using a comparison between the accumulation radar and the MCoRDS radar. The accumulation radar from 2011 is known to have only the GPS/UTC problem. The GPS/UTC problem is easily detectable by comparing the data to raster imagery, so the only correction that could be in error is the 0 or -1 second offset and this generally happens when there are no good features in or above the ice to align the accumulation and MCoRDS2 radars. GPS time corrections and frames where no good sync information was available are given in the vector worksheet of the Parameter Spreadsheet.

Two of the missions, SE Glaciers on 11 April 2011 and Helheim/Kanger/Midguard on 19 April 2011, suffered from radar configuration failures and about 40 dB of sensitivity was lost on the high gain channel. Short portions of these data are still good so the datasets are published, but most of the data are not useful.

3.4 Sensor or Instrument Description

As described on the [CReSIS Sensors Development Radar Page](#), the Multichannel Coherent Radar Depth Sounder operates over a 180 to 210 MHz frequency range with multiple receivers developed for airborne sounding and imaging of ice sheets. Measurements are made over two frequency ranges: 189.15 to 198.65 MHz, and 180 to 210 MHz. The radar bandwidth is adjustable from 0 to 30 MHz. Multiple receivers permit digital beamsteering for suppressing cross-track surface clutter that can mask weak ice-bed echoes and strip-map SAR images of the ice-bed interface. These radars are flown on twin engine and long-range aircraft including NASA P-3, Twin Otter (TO), and DC-8.

All radar and processing settings are stored in the MATLAB files. GPS time corrections and frames where no good sync information was available are given in the vector worksheet in the Parameter Spreadsheet.

4 REFERENCES AND RELATED PUBLICATIONS

Akins, Torry Lee. 1999. *Design and development of an improved data acquisition system for the coherent radar depth sounder*, Department of Electrical Engineering and Computer Science: Master's Thesis, University of Kansas.

Allen, Christopher, Lei Shi, Richard Hale, Carl Leuschen, John Paden, Benjamin Panzer, Emily Arnold, William Blake, Fernando Rodriguez-Morales, John Ledford, Sarah Seguin. 2011. Antarctic Ice Depth Sounding Radar Instrumentation for the NASA DC-8, submitted for publication to *IEEE Transactions on Aerospace and Electronic Systems*, August 2011.

Blake, W., J. Ledford, C. Allen, C. Leuschen, S. Gogineni, F. Rodriguez-Morales, Lei Shi. 2008. A VHF Radar for Deployment on a UAV for Basal Imaging of Polar Ice. *Geoscience and Remote Sensing Symposium*. IGARSS 2008. IEEE International, 4: IV-498-IV-501, doi: 10.1109/IGARSS.2008.4779767.

Byers, K. J. 2011. *Integration of a 15-Element, VHF Bow-Tie Antenna Array into an Aerodynamic Fairing on a NASA P-3 Aircraft*, Department of Electrical Engineering and Computer Science: Master's Thesis, University of Kansas.

Byers, Kyle J., A. R. Harish, Sarah A. Seguin, Carlton Leuschen, Fernando Rodriguez-Morales, John Paden, Emily Arnold and Richard Hale. 2011. A Modified Wideband Dipole Antenna for an Airborne VHF Ice Penetrating Radar, submitted to *IEEE Transactions on Instrumentation and Measurement*, June 2011.

Chuah, T. S. 1997. Design and Development of a Coherent Radar Depth Sounder for Measurement of Greenland Ice Sheet Thickness, *CReSIS Technical Report*, 151: 175.

Fujita, Shuji, Takeshi Matsuoka, Toshihiro Ishida, Kenichi Matsuoka, and Shinji Mae. 2000. A Summary of the Complex Dielectric Permittivity of Ice in the Megahertz Range and its Application for Radar Sounding of Polar Ice Sheets. *Physics of Ice Core Records*, (185-212). T. Hondoh, Editor. Hokkaido University Press, Sapporo.

Gogineni, S., T. Chuah, C. Allen, K. Jezek, and R. K. Moore. 1998. An Improved Coherent Radar Depth Sounder, *Journal of Glaciology* 44(148): 659-669.

Gogineni, S., D. Tammana, D. Braaten, C. Leuschen, T. Akins, J. Legarsky, P. Kanagaratnam, J. Stiles, C. Allen, and K. Jezek. 2001. Coherent Radar Ice Thickness Measurements Over the Greenland Ice Sheet, *Journal of Geophysical Research-Atmospheres* 106(D24): 33761-33772.

Li, Jilu, John Paden, Carl Leuschen, Fernando Rodriguez-Morales, Richard Hale, Emily Arnold, Reid Crowe, Daniel Gomez-Garcia and Prasad Gogineni. 2011. High-Altitude Radar Measurements of Ice Thickness over the Antarctic and Greenland Ice Sheets as a part of

Operation Ice Bridge, submitted to *IEEE Transactions on Geoscience and Remote Sensing*, September 2011.

Lei Shi, C. T. Allen, J.R. Ledford, F. Rodriguez-Morales, W. A. Blake, B. G. Panzer, S. C. Prokopiack, C. J. Leuschen, and S. Gogineni. 2010. Multichannel Coherent Radar Depth Sounder for NASA Operation Ice Bridge, *Geoscience and Remote Sensing Symposium (IGARSS)*, IEEE International, (1729-1732), doi: 10.1109/IGARSS.2010.5649518.

Leuschen, Carl, Chris Allen, Prasad Gogineni, Fernando Rodriguez, John Paden, and Jilu Li. 2011, updated current year. *IceBridge Snow Radar L1B Geolocated Radar Echo Strength Profiles*, [list dates of data used]. Boulder, Colorado USA: National Snow and Ice Data Center. Digital media.

Leuschen, Carl, Chris Allen, Prasad Gogineni, Fernando Rodriguez, John Paden, Jilu Li. 2011, updated current year. *IceBridge MCoRDS L2 Ice Thickness, Surface, and Bottom*, [list dates of data used]. Boulder, Colorado USA: National Snow and Ice Data Center. Digital media.

Leuschen, Carl, Chris Allen, Prasad Gogineni, Fernando Rodriguez, John Paden, and Jilu Li. 2011, updated current year. *IceBridge MCoRDS L3 Gridded Ice Thickness, Surface, and Bottom*, [list dates of data used]. Boulder, Colorado USA: National Snow and Ice Data Center. Digital media.

Namburi, S. P. V. 2003. *Design and Development of an Advanced Coherent Radar Depth Sounder*, Department of Electrical Engineering and Computer Science, Master's Thesis, University of Kansas.

Paden, John, Christopher Allen, Sivaprasad Gogineni, Kenneth Jezek, Dorthe Dahl-Jensen, and Lars Larsen. 2005. Wideband measurements of ice sheet attenuation and basal scattering, *IEEE Geoscience and Remote Sensing Letters*, 2(2).

Paden, J. 2006. *Synthetic Aperture Radar for Imaging the Basal Conditions of the Polar Ice Sheets*, Department of Electrical Engineering and Computer Science, PhD Dissertation, University of Kansas.

Paden, J., T. Akins, D. Dunson, C. Allen, and P. Gogineni. 2010. Ice-sheet bed 3-D tomography, *Journal of Glaciology* 56(195): 3-11.

Player, K., Lei Shi, Chris Allen, Carl Leuschen, John Ledford, Fernando Rodriguez-Morales, William Blake, Ben Panzer, and Sarah Seguin. 2010. A Multi-Channel Depth-Sounding Radar with an Improved Power Amplifier, *High-Frequency Electronics*, October 2010: 18-29.

Rodriguez-Morales, F., P. Gogineni, C. Leuschen, C. T. Allen, C. Lewis, A. Patel, L. Shi, W. Blake, B. Panzer, K. Byers, R. Crowe, L. Smith, and C. Gifford. 2010. Development of a Multi-Frequency Airborne Radar Instrumentation Package for Ice Sheet Mapping and Imaging, *Proc. 2010 IEEE Int. Microwave Symp.*, Anaheim, CA, 2010: 157 – 160.

Shi, Lei, C. T. Allen, J. R. Ledford, F. Rodriguez-Morales, W. A. Blake, B. G. Panzer, S. C. Prokopiack, C. J. Leuschen, and S. Gogineni. 2010. Multichannel Coherent Radar Depth Sounder

for NASA Operation Ice Bridge, *Geoscience and Remote Sensing Symposium (IGARSS), 2010 IEEE International*, 25-30 July 2010: 1729-1732, doi: 10.1109/IGARSS.2010.5649518.

4.1 Related Data Collections

[IceBridge MCoRDS L2 Ice Thickness](#)

[IceBridge MCoRDS L3 Gridded Ice Thickness, Surface, and Bottom](#)

[IceBridge Accumulation Radar L1B Geolocated Radar Echo Strength Profiles](#)

[IceBridge Ku-Band Radar L1B Geolocated Radar Echo Strength Profiles](#)

[IceBridge Snow Radar L1B Geolocated Radar Echo Strength Profiles](#)

4.2 Related Websites

[CReSIS website](#)

[CReSIS Sensors Development Radar web page](#)

[IceBridge data website at NSIDC](#)

[IceBridge website at NASA](#)

[ICESat/GLAS website at NASA Wallops Flight Facility](#)

[ICESat/GLAS website at NSIDC](#)

5 CONTACTS AND ACKNOWLEDGEMENTS

Carl Leuschen, Prasad Gogineni, Fernando Rodriguez, John Paden, Chris Allen

The Center for Remote Sensing of Ice Sheets

Department of Electrical Engineering and Computer Science

University of Kansas

Lawrence, Kansas, USA

Acknowledgments:

The radar depth sounder data and data products from Center for Remote Sensing of Ice Sheets (CReSIS) have been collected on an ongoing basis since 1993 using grant funding from NASA and NSF. The most recent data were collected as part of the NSF Science and Technology Center grant (ANT-0424589) and the NASA Operation IceBridge field campaign (NNX10AT68G).

CReSIS faculty, staff, and students designed, developed, operated, and processed data from the radar systems.

6 DOCUMENT INFORMATION

6.1 Publication Date

November 2011

6.2 Date Last Updated

February 2019